

# Spines Spines Spines! Wonderful Spines!

Olivier Gemin<sup>1‡</sup>, Pablo Serna<sup>1,2,3,4\*Ⓢ</sup>, Nora Assendorp<sup>1</sup>, Matteo Fossati<sup>1</sup>, Philippe Rostaing<sup>1</sup>, Cécile Charrier<sup>1</sup>, Vincent Hakim<sup>2,3,4Ⓢ</sup>, Antoine Triller<sup>1‡</sup>

**1** Institut de Biologie de l'Ecole normale supérieure (IBENS), Ecole Normale Supérieure, CNRS, INSERM, PSL Research University, 75005 Paris, France

**2** Laboratoire de physique statistique, Département de physique de l'ENS, École normale supérieure, Université Paris Diderot, UPMC Univ. Paris 06, CNRS, PSL Research University, 75005 Paris, France

**3** Sorbonne Universités, UPMC Univ. Paris 06, École normale supérieure, Université Paris Diderot, CNRS, Laboratoire de Physique Statistique (LPS ENS), 75005 Paris, France

**4** Université Paris Diderot, Sorbonne Paris Cité, Laboratoire de Physique Statistique de l'ENS (LPS ENS), École normale supérieure, UPMC Univ. Paris 06, CNRS, 75005 Paris, France

ⓈThese authors contributed equally to this work.

‡These authors also contributed equally to this work.

\* serna@biologie.ens.fr

## Abstract

## Author summary

Spines are beautiful as they are.

## Introduction

### Dendritic spines

**What they are. Where do you find them. When they were discovered:**

Dendritic spines are small protuberances that appear in many kinds of neurons. They have associated a excitatory synapse. They are considered as individual units of computation for the neuron. Their inputs will be integrated later on their dendritic branch (shaft?) before reaching the soma.

**What their function is.** Functionality of spines have been subjected to lots of speculative hypothesis due to their small size. Whether they become electrical or chemical relatively isolated compartments, due to long and thin necks, or their functions for the plasticity of the synapse they harbor.

**What things are on the edge of knowledge.** Even if excitatory inputs usually ends in spines. It has been thought until very recently (2007 ?) that inhibitory synapses, such as GABAergic ones, could only contact dendrites in their branch. Theoretically it had even been predicted that an inhibitory synapse contacting a spine would be utterly useless. Yet there are some. They have been found in pyramidal neurons in L2/3 cortex in mice, as well as in cultured cells. They have also been identified in human cortex. They always appear with an excitatory synapse in the same spine. They account for



implies that this approximation would probably hold (for very large currents!?).

**Electrotonic hypothesis or multicompartment models.** A final step in simplifying the model, is assuming that the ionic concentration in the intracellular medium remain constant and the medium can be treated as a conductor (a cable) with a given conductivity/resistivity that depends on their mobility and charge. In general, this assumption can lead to wrong interpretation if it is considered for the whole neuron, since small compartments can get electrochemically isolated (REF:Higley y colleagues). However, a useful strategy consists in subdividing the neuron in smaller interconnected compartments where this approximations holds (REF:Rall and Demas), leading to the acknowledged multi-compartment models. A compartment can be considered as a block where the membrane may have specific properties, e.g., active conductances, synapses, etc. The assembly of this blocks makes the model of the neuron.

In general, this **electrotonic** hypothesis (???) works well and can be used when the dimension and amplitude of currents are within ranges where the electroneutrality hypothesis holds. For the range of currents we consider in this paper, the electrophysiological range, this is indeed the case (REF to future work).

**Top-down approach.** The building block of the model will be a cylindrical compartment with passive membrane properties determined from validated electrophysiological models (check methods). Each type of compartment may include different densities of active conductances and synaptic inputs. **(already said 2 paragraphs above..?)** Dendritic branches and spines will all include voltage-dependent calcium currents (VDCC) and when required inhibitory synaptic inputs (methods). Dendritic spines will also include at least an excitatory synaptic input (methods), which comprises both AMPAR and NMDAR mediated currents. In section (?), we will consider the same model and simulated experiments when we consider the compartments with active conductances, both to generate action potentials (AP) and nonlinear membrane responses.

## Baseline model

The intrinsic heterogeneity in the features that characterize spines is a hallmark of biological system. Despite this, in the literature this has been circumvented when modelling spines, due to the level of complexity introduced. We examine the effects of this heterogeneity in a multi-compartment model of the membrane of the neuron (ref: Rall, Segev, HH). The baseline (ground zero) model is sketched in panel a of Fig.1. In its simplest form, it comprises a compartment representing the soma, at least two dendrites and the spines that we may include in one of the dendrites. The dendrite that harbours the spine under study is subdivided in at least three sequential pieces, where the central one is connected to the spine. For more details, check the methods.

To include the different spine features we resample the data set, partially shown in previous section. Instead of using only those 375 spines we have analysed, we bootstrap the distribution – generating spines with similar characteristics and correlations (methods). Bootstrapping the data avoid missing intrinsic correlations in the data that can pass unobserved even with a careful analysis.

For each given spine in the bootstrapped data set, we simulate a glutamate release and estimate the membrane depolarization in different compartments (panel b of Fig.1). In blue we show the depolarization in the membrane of the spine head, where the solid line represents the median of the distributions of EPSPs. The shaded regions represents the 66% region interval. This can be compared with EPSPs registered in the soma, where the signal has been filtered by the dendrite, and thus has a slower kinetics,

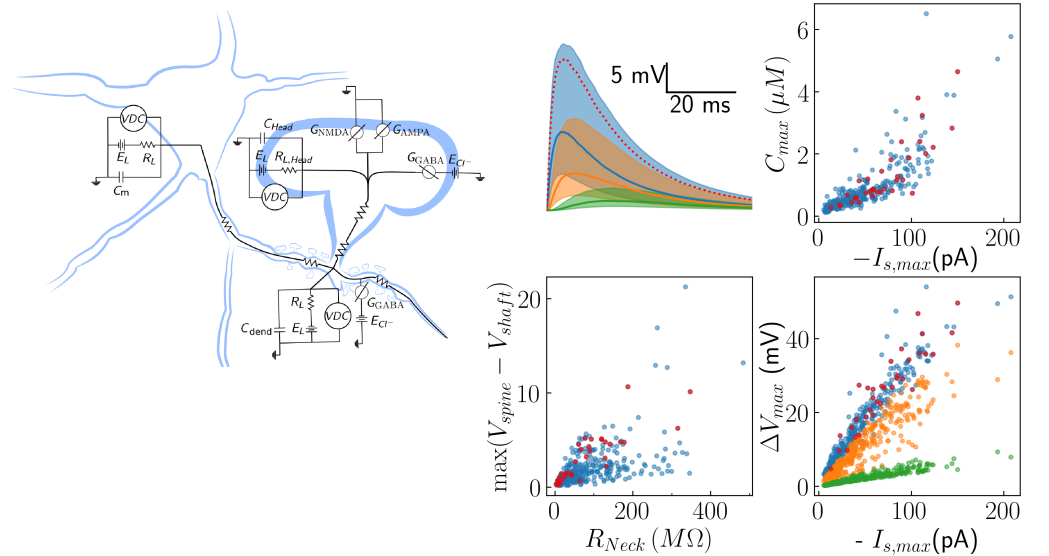


**Fig 1.** Panel **a** shows sketch of circuit model used for ..... each compartment includes passive membrane properties, active conductances such as Voltage dependent Calcium currents, etc. Inside the spine, the model includes an excitatory synapse with both AMPA and NMDA currents and the possibility of having second innervation with a GABAergic synapse. Inhibitory synapses can be located in the dendritic shaft or in the spine neck as well. Panel **b** shows the depolarization produced in the membrane of the spine head (blue) and in the dendritic shaft **30  $\mu m$  away!** (orange), when (only) glutamate release is simulated. Panel **c** shows the depolarization of the dendritic shaft and the soma in the same scenario. Panel **d** shows the amplitude of the depolarization in the ensemble of spines as a function of the amplitude of the current. Panel **e** shows the effects of the EPSP in the intracellular Calcium in the previous scenario (blue) and when NMDA currents is blocked (orange).

and the average amplitude of the EPSP is roughly 2 mV. We also plot, for comparison, the EPSP estimated 30  $\mu\text{m}$  from the spine (between the spine and the soma). (The behaviour with the distance will be analysed in the context of dendritic integration **below**.) The spread of the distribution is reflected in a large shaded area for EPSPs responses. **TO ADD**.- DiS are on higher part of the distribution, and are flagged as red?

The amplitude of the depolarization in the spine head compared to the one in its dendritic shaft depends linearly with the resistance of the neck, as shown in panel c, where other geometrical parameters generate 'normal' noise (???Check?: also **check main source of noise**). However, the amplitude of the EPSP is primarily driven by the synaptic current, in other words, the ePSD area (panel d). This is obviously not only in the spine, but it gets reflected in the other compartments too. Similarly, the amplitude of intracellular Calcium concentration depends mostly on the NMDA component of the synapses (**percentage coming from VDCC?**) – we assume this scale with area of the ePSD too. The component coming from VDCC is small (refs) and we fit the model to have a similar fraction in average  $\sim 30\%$ . A more thorough study of the effects on the variance of the signal is described in the appendix.

### DiS - Inhibition in spines

To assess the effects of DiS and their heterogeneity, we bootstrap the subset of DiS. In particular, we focus on the effects of axo-spinal inhibition compared to axo-dendritic inhibition. We assume the density of GABA<sub>A</sub>Rs in inhibitory synapses is independent of their location (any ref?), and their strength is then set by their area. Note that due to the difference in size between the two types of synapses the results will show a combination of effects due to the geometry of the compartments and the strength of the synapses. We analyse this separately in the appendix.

One of the main effects of inhibition in the dendrite is to locally shunt the membrane when incoming EPSPs arrive (refs). This depends on the chloride reversal potential and resting potential of the cell. Although it changes during development and other conditions, we will consider here both at -70 mV. If inhibition and excitation are uncorrelated, the former only have an average effect reducing EPSPs. However correlated inhibition may have a much stronger effect. To test this, we include a inhibitory contact in the compartment of the spine head, panel a in Fig.2.

In panels b1 and b2 we show the effect of inhibition in the intracellular Calcium in the spine head. It features the distribution of Calcium transients due to an EPSP without inhibition in black, and in green when inhibition arrives 5 ms after (panel b1) or 5 ms before the EPSP (panel b2). The activation of the excitatory event is marked in red below the curves, while the inhibitory one is in green.

To study the effects for signal integration, we extract the amplitude of the Calcium and Voltage transients. In order to see the effect of inhibition, we normalise the amplitude to a case with no inhibition. In panel c, we show the in the spine head both for voltage (blue) and Calcium (orange), and for DiS (dark colors) and SiS with an inhibitory synapse nearby (lighter colors). When inhibition comes first, the GABAergic current has the chance of shunting the depolarization peak. In contrast, when it comes last (?) the effect on the amplitude disappears (except for a very small window of time). The asymmetry is manifest, but exhibits slower dynamics in Calcium compared to voltage. This is due to the slower dynamics of NMDAR-mediated currents, which account for most of Calcium entry in spine heads. The effect of inhibition inside the spine is clearly (???) different in DiS (dark colors) as compared to SiS (lighter colors).

The effect of the interplay of a single inhibitory and single excitatory input in the soma and in dendritic shaft are shown in panel f of Fig. 2. Similarly to the spine head (in panel e), the asymmetry appears for the depolarization as a function of the delay of

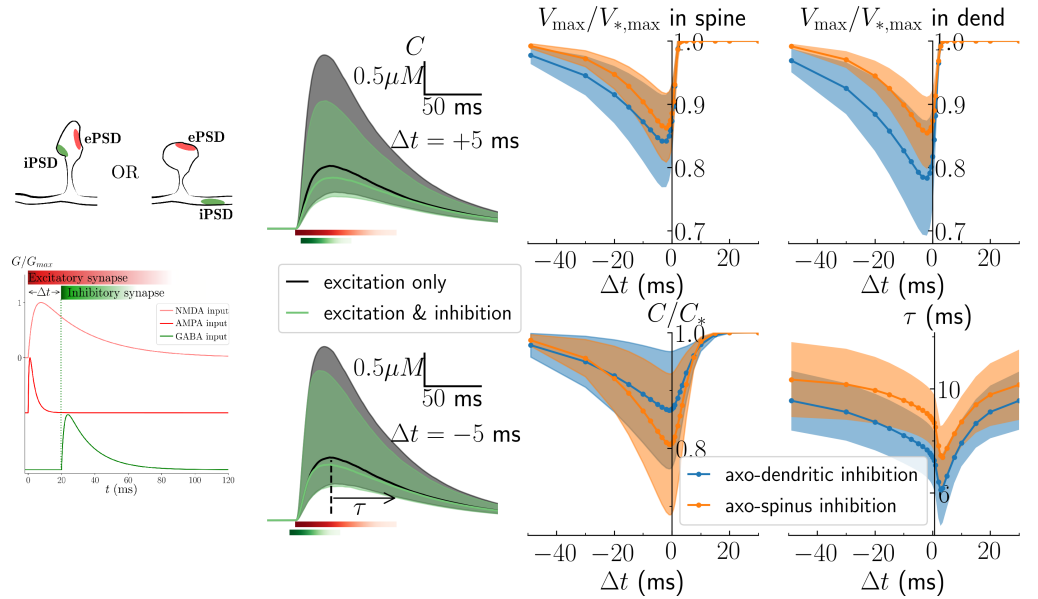


**Fig 2. Timing of inhibition.** Panel a show a sketch of the protocol for the timing of inhibition. In case I (black) a glutamate release is simulated at a (bs) DiS spine and after  $\Delta t$ , GABA release is simulated and inhibitory synapse is activated. In case II (violet) GABA is released first and after  $-\Delta t$  time glutamate is simulated. The effect on the depolarization in the spine head is shown in panel b1 when  $\Delta t = 15$  ms. Note that inhibition effect is shunting the membrane, so when it arrives first its effect is not apparent until glutamate arrives. In panel b2, the effect on the intracellular Calcium is shown. In panel c1 and c3, we show the the amplitude of the depolarization and calcium concentration as a function of  $\Delta t$  (negative values: GABA arrives first; positive values: glutamate arrives first), normalized to the case without inhibition. In panel c2, we show the decaying time of the depolarization as a function of  $\Delta t$ .

inhibition. However, there is no big(??) difference of the effect of inhibition depending on its location: in spine (dark blue) in the shaft closer to the soma (light green) or further from the soma (light purple) (there may be difference with this case - check).

### Dendritic integration - synaptic gating

**Attenuation of the signal.** Signal as a function of the distance. Electrotonic concept (Rall). Chirality broken (REFs?). Determination of the electrotonic length. Shunting Levels with inhibition along the dendrite: What happens with inhibition: in spine/ out of spine/ in dendritic branch (REF: paper journal club).

On this aspect of dendritic integration we can study how the effect depends on the distance to the synapse for both excitatory and inhibitory synapse. For the excitatory synapse is relatively straightforward, we compare the amplitude of the EPSP along the dendrite with the value in front of the spine. For the inhibitory synapse instead, the effect is usually shunting the membrane. For those cases when there is a hyperpolarization or a depolarization due to inhibition, the effect is rather small, and what would happen there – similar to excitation?? To define the effect of shunting we place the second spine at a distance  $x$  of the axo-spinal contact and elicit there an EPSP, with an amplitude without inhibition  $V_0$ . Now, we repeat the same experiment with axo-spinal inhibition arriving 5 ms before the EPSP (what happens if it is later? Nothing?). The decrease in amplitude of the latter,  $V_i(x) < V_0$ , is the shunting effect due to the inhibitory synapse. To quantify it we consider the difference of the two

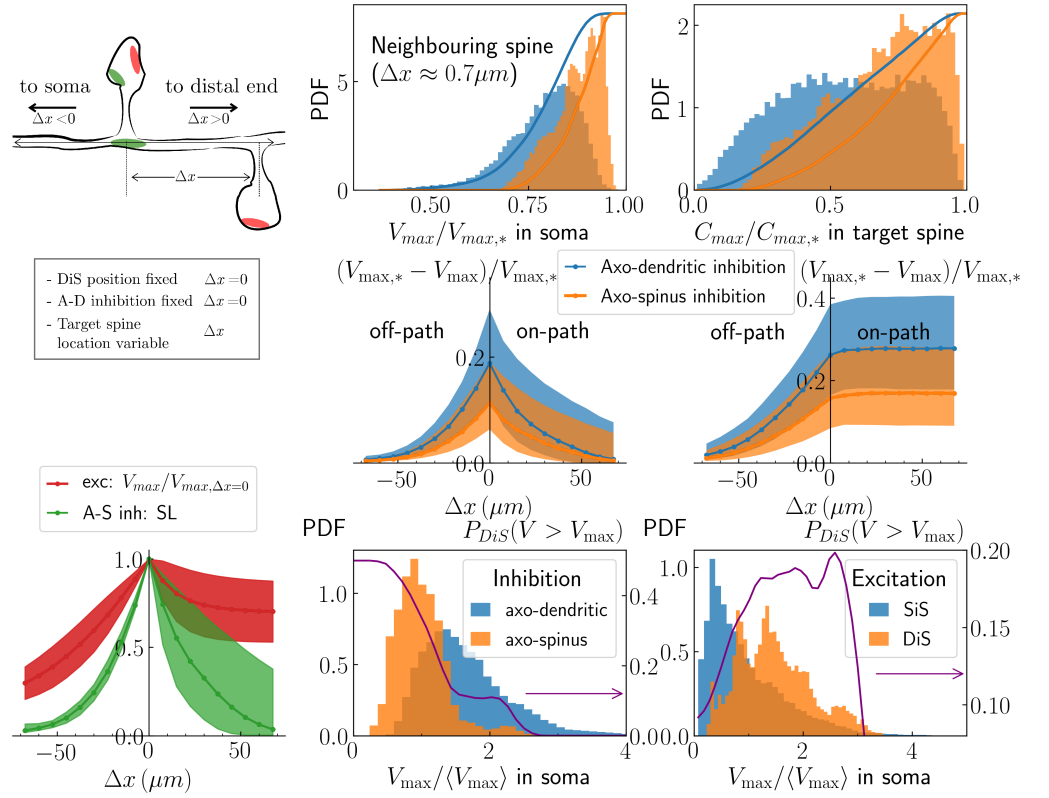


**Fig 3. Dendritic integration.** Panel a – sketch spines distance and interaction. Panel f – attenuation of the signal as a function of the distance to the synapse for both excitatory (red) and inhibitory synapses (green) in DiS.

amplitudes normalized to  $V_0$ . In panel d, we show the ratio of this quantity compared to having the spine next to the axo-spinal inhibitory contact

$$SL(x) = \frac{V_0 - V_i(x)}{V_0 - V_i(0)}$$

**Gating synapse.** An interesting phenomenon already described in the literature is synaptic gating (Ref). This refers to the fact that some inhibitory inputs may selectively gate excitatory inputs decreasing their amplitude. Inhibitory synapses in DiS might be an ideal candidate to drive it. We design a different protocol to address this problem, we consider two spines in a small piece of dendrite in the dendritic arbor we simulate. One of the spines is dually-innervated (the other is extrated from the whole set of spines). We simulate an EPSP incoming in the second spine and measure its effect in the soma or in the dendrite. This will be the control experiment. Then, we repeat it and have inhibition activated slightly before the EPSP in the DiS ( $\Delta t = -5 ms$ ). We show the histogram of the normalised depolarization amplitudes in the soma in panel b (very similar to the one observed in the dendrite). Similarly, we repeat this protocol, but activating an inhibitory synapse in the dendritic shaft instead of the one in the DiS. The distribution is shown in red. There is a clear shift, ???% vs ???%. Note that the fact that axo-dendritic synapses are larger than axo-spinal ones makes this difference stronger. In the case of similar sizes, the difference in the two effects is roughly ???% (appendix). The effect can be seen in the intracellular Calcium concentration in the spine head of the second spine, panel c. **(Is the difference in the median of the**

distribution the fact that we are sampling all the spines?). The shift in the median from axo-dendritic to axo-spinal inhibition is ??%. **Should we speak about literature inhibition and Calcium - Journal club.**

## STDP

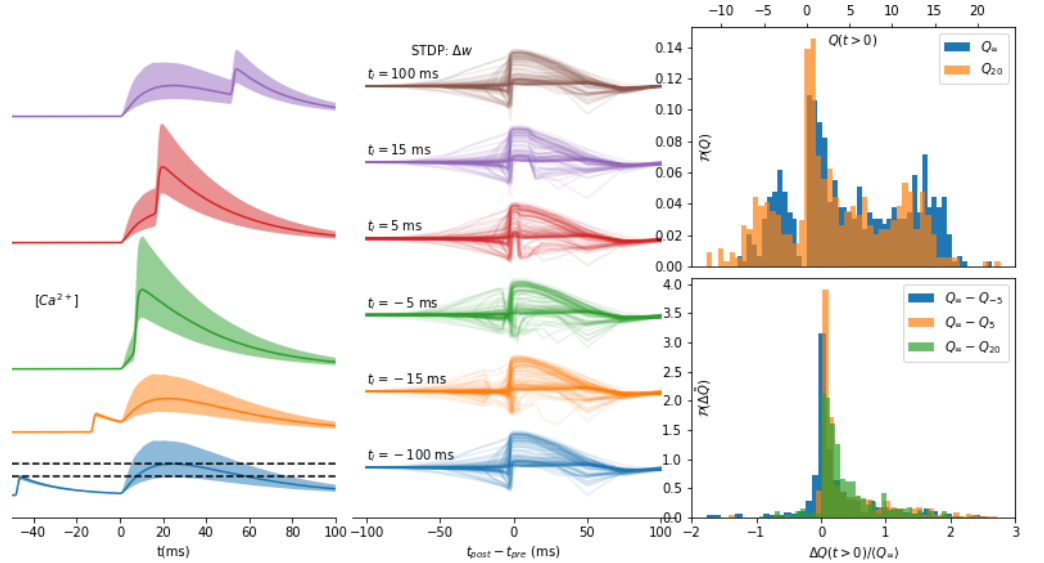


**Fig 4. STDPs.** Panel a shows Calcium transients for a STDP protocol for several cases of  $\Delta t_1$ , timing between (excitatory) pre- and postsynaptic AP. Panel b shows the heterogeneity of STDPs curves we obtain in a protocol of 100x 0.5 Hz. In panel c, colormap of 2  $\theta$  with probability of finding DPD curves. Panel d shows how inhibition changes STDPs curves for those typical DPD' curves found in SSx.

## Active conductances

This section includes modeling bAPs to model Hebbian STDP in DiS. Varying the timing between E/I stimuli (let alone the respective synaptic strengths, responsiveness and channel kinetics) will give insights on the fine regulation of Hebbian STDP by axo-spinal inhibitory synapses.

## Discussion / Conclusion

## Materials and methods

### Animals

All animals were handled according to protocols approved by French authorities. Timed-pregnant female mice were maintained in a 12 hr light/ dark cycle and obtained by overnight breeding with males of the same strain. For timed-pregnant mating, noon after mating is considered E0.5. Adults correspond to mice between P84 and P129.



## In utero cortical electroporation

In utero cortical electroporation was performed at E15.5 on timed pregnant RjOrl:SWISS females (Janvier Labs) for electrophysiology or C57BL/6J females Janvier Labs in Figure 5. The previously described protocol for in utero cortical electroporation (Hand and Polleux, 2011) was modified as follows. We used timed pregnant RjOrl:SWISS females. Endotoxin-free DNA was injected using a glass pipette into one ventricle of the mouse embryos. The volume of injected DNA was adjusted depending on the experiments. Electroporation was performed at E15.5 using a square wave electroporator (ECM 830, BTX) and gold paddles. The electroporation settings were: 4 pulses of 40 V for 50 ms with 500 ms interval.

## Tissue preparation

### A Methods

### B Bootstrap

The statistics of the set of measurements we have presented in this manuscript is non-trivial. We do not only refer to the appearance of log-normal like distributions, with not-so heavier tails, but also the existence of non-linear correlations between observables. Although some correlations can be modeled in a relative simple way, e.g., area vs volume of the spine head (REF? Yuste), in other cases it requires a bigger effort, e.g., **the figure with weird correlation 1/length: length vs volume or something like that (REF)**. Also, we are not interested in the effect of this particular snapshot of spines, but rather in the effect of generic spines that we have had access to, through the snapshot that we took. We use (smooth) bootstrap methods to re-sample the distribution with the correlations. We use the synthetically generated spines (that have similar statistical properties to those we physically measured) to sample the distribution of electrochemical effects in a neuron model environment.

**Bootstrap.** Bootstrap methods consist in re-sampling measured data in a random fashion. Our set of data consist in a matrix  $\mathcal{D}$  of dimension  $N \times N_O$ , with  $N = 370$  number of spines and  $N_O = 25$  number of observables. Note that some of the observables may not be used in the **simulations**. If we consider measurements of each spine completely independent, a simple bootstrapping technique to generate a new set  $\mathcal{D}'$  of  $M$  spines consists in selecting them randomly (with possible repetition) from the rows of  $\mathcal{D}$ . However, if we want to sample better the distribution of effects, we want to smear the distributions of parameters retaining its features. Even if there is correlation between variables, we will assume that the noise in each variable is small and independent from each other. To estimate the amount of noise we can introduce, let us study it in a particular example: the length of the neck.

We calculate first the (cumulative) distribution of the original set of length of spine necks  $\mathcal{L} = \{l_i, i = 1, \dots, 370\}$ , comprising 370 cases, Fig. 5. We bootstrap the data set by producing  $M = 500$  random indices from 0 to 370 (with repetition) and generating a new synthetic set  $\mathcal{L}' = \{l'_{j_1}, \dots, l'_{j_{500}} / l'_j = l_j(1 + \sigma\xi)\}$  where  $\xi$  is a random gaussian variable with variance 1 and  $\sigma$  the noise level. We calculate the distribution for  $\mathcal{L}'$  and perform a 2 sample Kolmogorov-Smirnov test, obtaining a  $p$ -value. We repeat this procedure 1000 times for each studied noise level and obtain statistics. In Fig. 5, we show for different noise levels the fraction of synthetic sets whose  $p$ -value is below various thresholds (color coded). Since we want to keep small noise levels as well, a noise level of  $\sigma = 0.1$  seems to avoid generating synthetic sets with  $p$ -value below 0.05, a lax constraint (to consider them different).

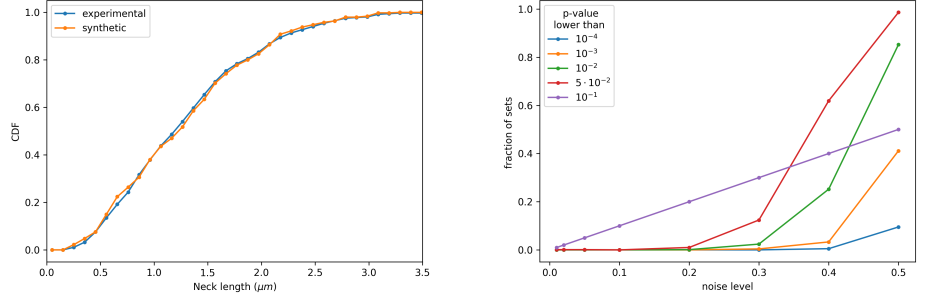


**Fig 5.** Panel a shows cumulative distribution of the experimental length of the spine necks compared to a synthetic set with noise level 0. 2 sample KS test gives a p-value of 0.95. Panel b shows fraction of spine sets whose neck length distribution produces a p-value lower than various thresholds, in a 2 sample KS test with the experimental distribution as a reference. This is shown as a function of the amount of gaussian noise introduced in smoothed kernel for bootstrap.

We have checked that  $\sigma = 0.1$  is a correct noise level for other quantities subjected to noise in their measurements. New synthetic spines are produced by choosing one index from 0 to  $N$  and introducing noise as gaussian random variables in each one of the selected variables (independently). Note that we do not select independently different features, by selecting  $N_O = 25$  random indices, with the aim of keeping the correlations associated to the system we have had access.

**Paragraph about the boons of bootstrapping!** DiS are very few, we now have many to play with. It can be used to test other stuff. What else? It gives an estimate of errors of the measurements as well. Anything else?

## References